

Stone pore imitating artificial test systems: current prototypes and potential for cultural heritage care

Andra-Lisa M. Hoyt, Helmut Cölfen
Physical Chemistry, University of Konstanz,
Universitätsstraße 10, 78464 Konstanz, Germany

Abstract

Cultural heritage made from carbonatic rocks suffers a multitude of deteriorating processes, including acidic influences by environmental pollution. Prominent examples include calcitic materials such as limestone and marbles – often used in architecture and sculpting.

Even among calcitic stone there are significant differences in porosity, wetting behavior and environmental conditions that must be considered to plan a successful and sustainable restoration or preservation. In addition to traditional treatments (e.g. limewater), nanolime dispersions like Nanorestore Plus® have become available in recent decades. Although quite successful in case studies, their mode of action inside pores is not yet fully understood and they are not ideally

suited for all applications. Major drawbacks include the necessity to adjust particle to pore sizes in order to achieve optimal results without white hazing or complete clogging of pores.

To optimize stone care efforts, it is crucial to understand infiltration, drying and crystallization of these remineralization solutions inside stone pores. While destructive and time-delayed investigations such as thin cuts or microdrilling are state of the art in the field, there is no widely used, fast and easily accessible way of following these processes *in situ* and real time.

A novel stone-pore-imitating microcomb test system (MCTS) has been developed that enables exactly this by providing an artificial transparent and constrained surrounding with tunable surface properties. This MCTS is used for infiltration studies of Nanorestore Plus® using light microscopy. Also, the potential of liquid mineral precursors as non-size-constrained restorative based on complex coacervation will be discussed. We propose a system containing a dense liquid phase of poly acrylic acid (common adhesive for stone) and calcium ions as future alternative to currently available treatments for limestone remineralization.

Keywords: calcite crystallization, infiltration, stone pores, remineralization, liquid mineral precursor

Introduction

Cultural heritage is one of the features that sets humans apart from other species on our planet. Many of these objects consist of stone with a high calcium carbonate (lime, CaCO_3) content and varying degrees of porosity. This makes them vulnerable to many decaying influences like flooding, wars, human error, or natural degradation processes (Steiger 2011). Water is involved in most of these and damage is exacerbated by the presence of acidic depositions leading to chemical dissolution (see Figure 1). A prominent example is acid rain caused by environmental pollution (Wellburn 1997). The importance of preserving this heritage has been stressed by many organizations and individuals.

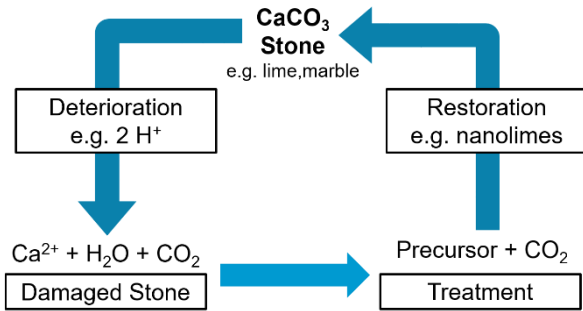


Figure 1: Demineralization/reminerzalization cycle of CaCO_3 .

Nevertheless, funding is often scarce and time of the essence before precious artifacts are lost.

Traditionally, highly calcitic rocks were treated with limewater (Peterson 1981), which has relatively low mineral content, necessitating a high number of applications, and introducing a lot of water into the artifact. Since the turn of the last century, nanolimes have been introduced and studied as promising and improved alternatives (Otero 2017, Otero 2018). Some nanolimes, like Nanorestore Plus® (NR+), have been commercialized. Their exact mode of action, however, is not yet fully understood and room for further improvements remains.

First, nanolimes are solid particle dispersions. Therefore, the size distribution of the particles and the pore size distribution of the substrate are crucial factors for the success of the treatment (Otero 2019). Oversized particles can clog small pores, while particles too small will migrate back to the surface and react too quickly. Both processes can potentially lead to undesirable white haze formation on the material surface instead of remineralization and recohension in deeper layers. Liquid mineral precursors from complex coacervation as alternative treatment for calcitic rocks could avoid these problems due to their non-solid nature (Kaempfe 2013). The principle of their formation is depicted in Figure 2. Adding calcium (Ca) ions to an aqueous solution containing a poly(anionic acid) leads to local liquid-liquid phase separation resulting in droplets that grow over time until complete phase separation occurs (Kaempfe 2013). Droplet growth can be arrested anytime by adding a suitable anion, e.g. carbonate to create size-

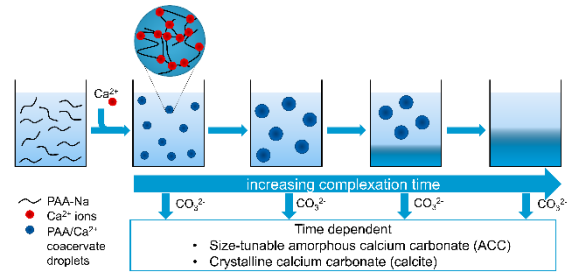


Figure 2: The principle of complex coacervation using a poly anionic acid sodium salt (PAA-Na) and Ca ions (Ca^{2+}) based on the synthesis first proposed by Kaempfe (2013) and adapted.

tunable amorphous or crystalline CaCO_3 particles. Typical indicators for successful synthesis of complex coacervates (CC) include turbidity, liquid-liquid phase separation, and increasing droplet sizes over time.

Secondly, there currently is no standard method for investigating the mode of action of treatments in real-time directly inside pore spaces. State of the art are time delayed and/or destructive methods like thin cuts and drill resistance measurements (Delgado Rodrigues 2018) or investigations on flat surfaces (Baglioni 2014). A transparent artificial pore-imitating test system called MCTS (micro comb test system) for stone related research questions has been developed in recent years (Gruber 2017).

This paper presents preliminary results concerning the analysis of CC as liquid CaCO_3 precursor and their potential use as restoratives, as well as infiltration experiments with NR+ and the liquid precursors using the MCTS.

Methods

Complex coacervates: 10 mL aqueous *calcium chloride dihydrate* ($\geq 99\%$, Sigma-Aldrich) solution was added to 10 mL aqueous *poly(acrylic acid) sodium salt* solution (PAA-Na, 15 kDa, 35 w% in water, Sigma-Aldrich) in a 50 mL reaction flask and stirred at 750 rpm for four minutes after mixing. For mineralized solutions 10 mL *sodium carbonate* ($\geq 99.8\%$, Sigma-Aldrich) solution was added 2 minutes after mixing of the first two components. *Hydrochloric acid* (37%, VWR) and *sodium hydroxide* (1N,

Merck) solutions were used for pH modifications of the reagent solutions prior to mixing. Test System (MCTS): Photolithography using a negative photo resin. Tuned to *Pietra Serena* (PS) and *Carrara Marble* (CM) wetting properties as described by Gruber (2017). Infiltration: NR+ 5 g/L in ethanol as purchased from CSGI (Florence). 0.5 mL of the respective solutions were used in the experiments and applied every 24 h (six times total) via syringe to the test system reservoir. Test systems were stored at 80 ± 5 % relative humidity and 20 ± 2 °C. Observation: directly after infiltration and after 24 h of drying. Polarized light microscopy (PLM): transmitted light on *Zeiss Imager M2Mm* with *Zeiss AxioCam MRc5* and *ZEN* software. Dynamic light scattering (DLS): Malvern *ZetaSizer ZSP* and software. Graphs: smoothed with the b-spline function of *Origin* software. pH values: Metrohm *691 pH Meter*. Water: double deionized water from MilliQ Direct 8 Machine from Merck Millipore (Darmstadt, Germany).

Liquid Calcium Carbonate Precursors from Complex Coacervation

The synthesis procedure was based on the original publication by Kaempfe (2013) and modified. Ca source and PAANa were each dissolved in water at different concentrations: 0.2 M and 1 M for Ca, 0.5 mg/mL and 1 mg/mL for PAANa. Each solution was adjusted to four different pH values (6, 7, 8, 9). Only solutions of the same pH were

mixed. Instead of using a flow reactor for combination as done by Kaempfe (2013) components were mixed in a small flask using a magnetic stirrer. In a separate series, sodium carbonate solution (unaltered pH) was added to the mixtures for mineralization. 16 mixtures each (4 pH values * 4 solution combinations) were investigated for unmineralized and mineralized series. For these mixtures, the following could be observed:

At pH 8 and 9 solutions containing the higher calcium concentration completely destabilized only a few minutes after combination resulting in low to no turbidity (see Figure 3A). The same is true for samples of all pH values containing a lot of calcium and only a little PAANa. Sufficient ratios of PAANa to calcium seem to be essential for dispersion stability. For low concentrations of both components, the turbidity of the sample increased from pH 6 to pH 9 (see Figure 3B). Highest overall turbidities resulted from mixtures with high PAANa and low calcium concentrations. Mineralized solutions followed the same trends, but all sedimented within hours of preparation. Clear liquid droplets surrounded by the aqueous phase were visible on the bottom of the flasks with unmineralized solutions after about 24 h (see Figure 3E).

The most promising sample for stone treatment was prepared using both low calcium and PAANa content solutions at pH 8. It exhibited comparably high turbidity (indicating plentiful scattering droplet formation) at moderate pH (neither too

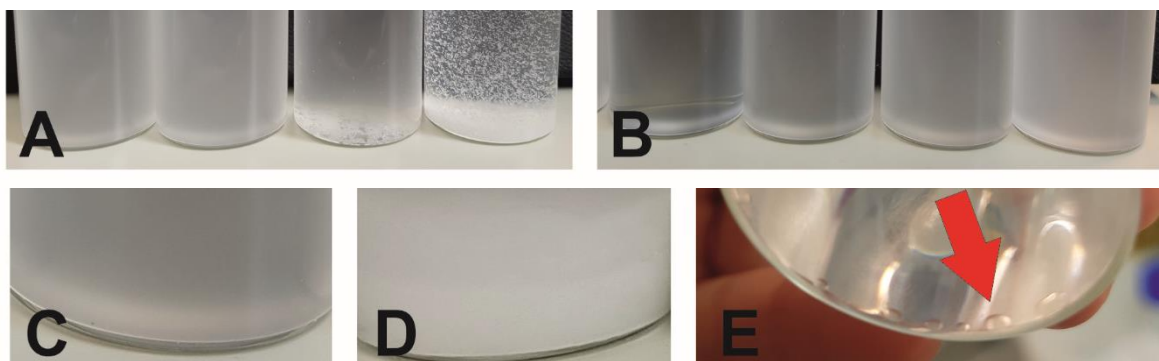


Figure 3: (A) Mixtures of high PAANa and Ca content at pH 6-9 (left to right) shortly after mixing. (B) Mixtures of low PAANa and Ca content at pH 6-9 (left to right) shortly after mixing. (C) Mixture of low PAANa and Ca content at pH 8 shortly after mixing. (D) Mineralized mixture of low PAANa and Ca content at pH 8 about 1.5 h after mixing. (E) Mixture from Image C about 24 h later.

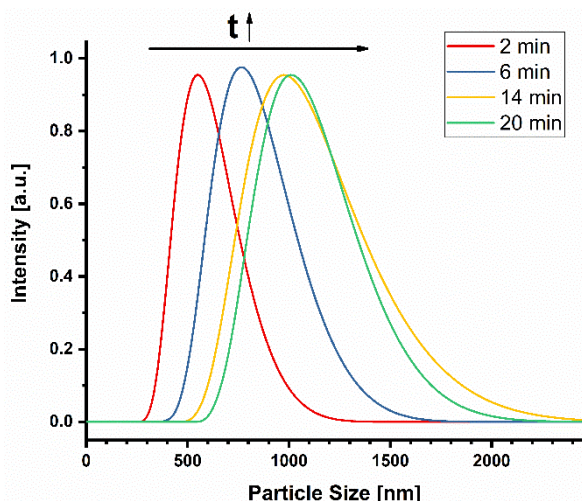


Figure 4: Number-weighted DLS particle size distribution (normalized) of CCS (0.2 M Ca ions, 0.5 mg/mL PAANa) over time.

acidic to do damage nor too alkaline to precipitate too fast with carbon dioxide from the air) with good stability in mineralized and unmineralized state (see Figures 3C and 3D). At the same time, PAANa content (technically an impurity in the artifact later) is low and mineral content acceptable (high mineral content means less applications for same remineralization material introduction). This formulation was used for all further experiments.

To verify the continuous growth of the droplets in the solution the sample was investigated using dynamic light scattering (DLS) immediately after mixing (Figure 4). The experiment was performed multiple times on the same unmineralized complex coacervate solution (CCS) sample. For the first three distributions a clear size increase over time from about 600 to over 1000 nm occurred. The growth seems to be complete within 20 minutes after mixing. Averaged diameters of the scattering droplets are given in Table 1. They all follow the same trend and are comparatively similar considering their standard deviations.

Table 1: DLS data from Figure 4 including time t since sample mixing, z -averaged diameter d_z , poly dispersity index PDI, intensity-weighted diameter d_i , and number-weighted diameter d_n . Standard deviation denoted as σ .

Measurement	t [min]	d_z [nm]	PDI	d_i [nm]	σ_{d_i} [nm]	d_n [nm]	σ_{d_n} [nm]
1 (red)	2	624	0.025	644	138	584	140
2 (blue)	6	869	0.118	877	178	807	184
3 (yellow)	14	1210	0.200	1186	290	1056	276
4 (green)	20	1323	0.327	1136	211	1065	222

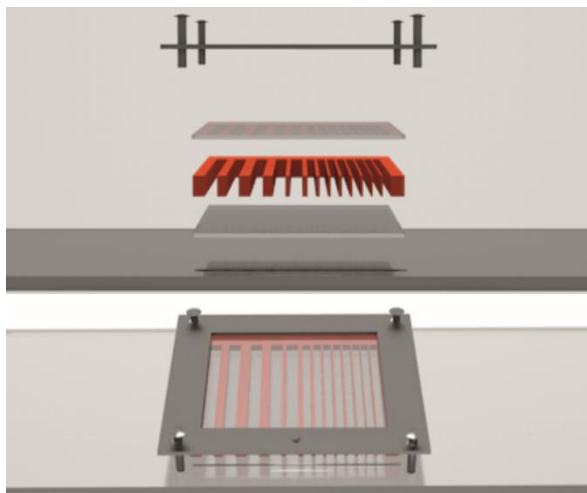


Figure 5: Schematic of the disassembled (top) and assembled (bottom) MCTS, as described by Gruber (2017).

In conclusion, the criteria for successful synthesis of CC were satisfied for a number of the investigated mixtures.

Infiltration of Restoratives and Solvents

The MCTS (see Figure 5) was prepared and attuned to the surface properties of *Pietra Serena* (PS) and *Carrara Marble* (CM) following the methods described by Gruber (2017). PS- and CM-tuned MCTS were infiltrated with either NR+ in ethanol or the most promising CCS. For images: golden areas are microcomb teeth, spaces in between are pores. Bottom of the image is the infiltration edge. Colored particulates are refracting material (crystalline).

For NR+ infiltration into both tuned systems, deposited crystalline material was visible already after the first infiltration and drying cycle using PLM. Small particles were visible coating the sides of the channels and capping the open teeth ends for channel widths from 100 to 300 μm (see Figure 6, top row). The coating layer was thickest around the open ends of the pores and thinned towards the closed back end of the pores. After six infiltrations and 24 h of drying the amount,

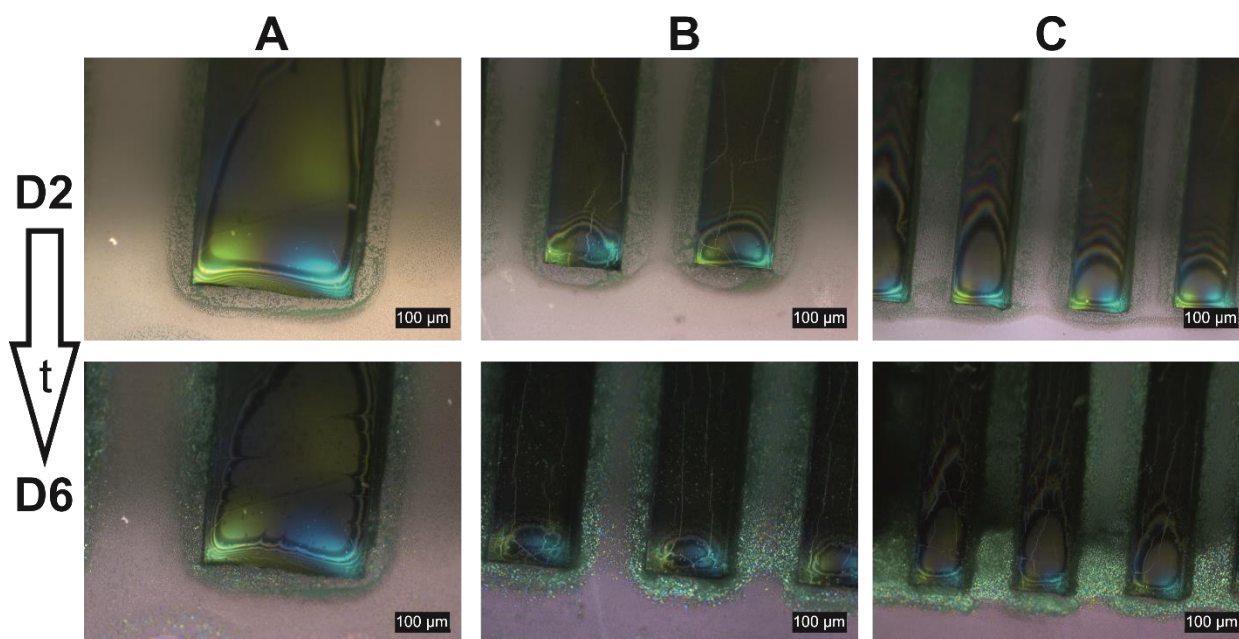


Figure 6: PLM images of PS-tuned MCTS infiltrated with NR+. Top row: after two infiltrations and 24 h of drying. Bottom row: after six infiltrations and one day of drying. Columns: Teeth / pores of width 300 μm (A), 150 μm (B), 100 μm (C).

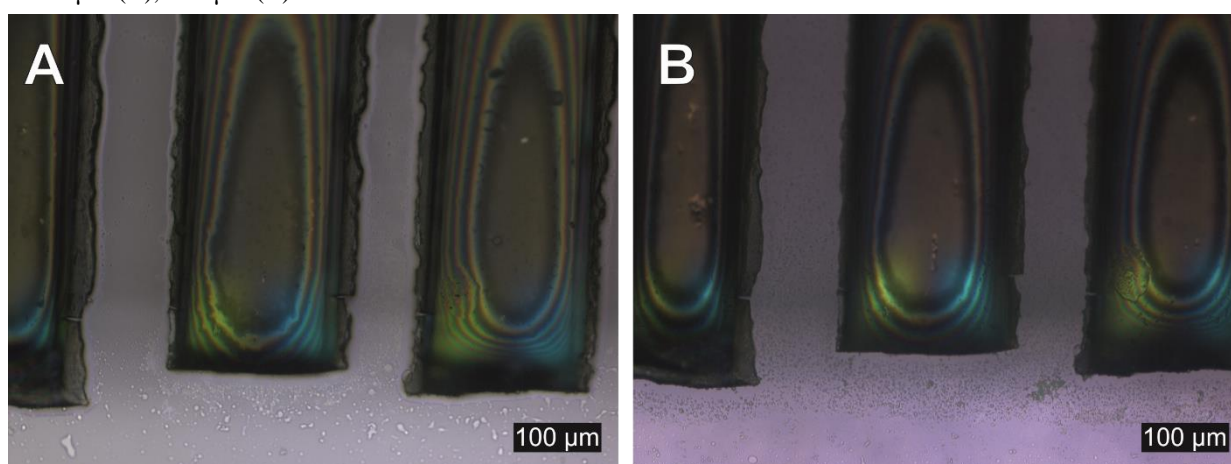


Figure 7: PLM images of PS-tuned MCTS infiltrated with a CCS. Pore and teeth width of 150 μm each. (A) MCTS after three infiltrations and one day of drying. (B) Same MCTS after six infiltration cycles and additional 17 days of drying.

size and crystallinity of deposited material is increased (see Figure 6, bottom row). Capping of the open ends and thinning of the coating layer towards the back was also observable. The smallest channels are covered completely by crystalline material and the second largest pores are partially bridged at the open pore ends while the channel further back remains only coated. The largest pores remain open. For the PS-tuned system, the coating of the channels was very regular and even compared to slightly more local clustering of particles in the coating layer for the CM-tuned MCTS. The crystallinity and particle size of deposited material seemed slightly higher

for PS-tuned systems. After six infiltrations of fresh CCS into a PS-tuned MCTS and 24 h of drying, amorphous liquid droplets of varying dimensions were visible in the whole channel and along the infiltration edge (see Figure 7A). A liquid film can be observed coating the channel walls. After storage for another 17 days the droplets at the open end of the pores have been replaced by very finely spread small refracting particulates. Deeper into the channels this has not taken place everywhere and more amorphous liquid droplets remain (see Figure 7A). As pure water should have long evaporated, the continued presence of liquid droplets indicates the presence

of the denser CC fluid.

Overall, NR+ deposits a larger amount of bigger crystalline particles in less application cycles than the CCS. NR+ only coats the sides of the channels, though, and tends to clog pore entrances without filling up channels evenly, while the complex coacervate treatment leads to finer, smaller crystalline particulates regularly spread over the whole channel.

Summary and Outlook

Of the investigated CC formulations almost all mixtures exhibited the typical increase in turbidity upon mixing of the components and many were stable for several hours. Some turbidity trends related to pH and concentration ratios were observed. All unmineralized formulations showed the expected liquid-liquid phase separation over time and growth of the contained scattering entities was demonstrated. Successful synthesis of CCS from Ca ions and PAA using our modified synthesis method was achieved.

The MCTS was successfully used to observe infiltration, drying and crystallization of NR+ and the CCS. Some notable differences in coating and crystallization behavior were observable. This is a qualitative comparison only but already points to CC potentially providing a different restorative performance that may be better suited for many other substrates or treatment goals.

Next steps include further optimization of the CCS to higher Ca and lower PAANA content. Also, applying the pure separated droplet phase should be explored to further limit water contact of treated substrates. Issues with the MCTS such as leakage, breakage, non-carbonatic surface functional groups and high smoothness untypical for natural stone must all be addressed in future versions of the test systems. Possible options include microfluidic chips made from polymethylmethacrylate (PMMA) or polydimethylsiloxane (PDMS). Additionally, quantitative evaluation of the infiltration experiments is needed to improve our insight into remineralization performance and to reliably compare different products. More studies will be

performed with both the test system and natural stone samples to verify and directly compare the results.

In the future, destructive stone sample collections for infiltration testing before treatment may well become a thing of the past – or at least be greatly reduced.

We thank the Deutsche Bundesstiftung Umwelt (DBU), nano.lab and workshop of Konstanz University, and the Deutsche Forschungsgemeinschaft DFG (SFB-1214 project Z1).

References

- Baglioni, P., D. Chelazzi, R. Giorgi, E. Carretti, N. Toccafondi, Y. Jaidar 2014. Commercial Ca(OH)₂ nanoparticles for the consolidation of immovable works of art. *Appl Phys a-Mater* 114(3):723-732.
- Delgado Rodrigues, J., A. P. Ferreira Pinto, R. Nogueira, A. Gomes 2018. Consolidation of lime mortars with ethyl silicate, nanolime and barium hydroxide. Effectiveness assessment with microdrilling data. *J Cult Herit* 29:43-53.
- Gruber, D., S. L. P. Wolf, A.-L. M. Hoyt, J. P. Konsek, H. Cölfen 2017. A Micro-Comb Test System for In Situ Investigation of Infiltration and Crystallization Processes. *Minerals* 7(10):187.
- Kaempfe, P., V. R. Lauth, T. Halfer, L. Treccani, M. Maas, K. Rezwan 2013. Micromolding of Calcium Carbonate Using a Bio-Inspired, Coacervation-Mediated Process. *J Am Ceram Soc* 96(3):736-742.
- Otero, J., A. E. Charola, C. A. Grissom, V. Starinieri 2017. An overview of nanolime as a consolidation method for calcareous substrates. *Ge-conservación* 1(11):71-78.
- Otero, J., V. Starinieri, A. E. Charola 2018. Nanolime for the consolidation of lime mortars: A comparison of three available products. *Constr Build Mater* 181:394-407.
- Otero, J., V. Starinieri, A. E. Charola 2019. Influence of substrate pore structure and nanolime particle size on the effectiveness of nanolime treatments. *Constr Build Mater* 209:701-708.
- Peterson, S. 1981. Lime water consolidation. Mortars, cements and grouts used in the conservation of historic buildings. Symposium, Rome, 3-6 Nov., 53-61.
- Steiger, M., A. E. Charola, K. Sterflinger 2011. Weathering and Deterioration. In: S. Siegesmund and R. Snethlage (eds) *Stone in Architecture: Properties, Durability*. Berlin, Heidelberg, Springer, 227-316.
- Wellburn, A. R. 1997. Saurer Regen. In: (eds) *Luftverschmutzung und Klimaänderung: Auswirkungen auf Flora, Fauna und Mensch*. Berlin, Heidelberg, Springer, 109-136.